N73 33184

NASA TECHNICAL MEMORANDUM

NASA TM X-71457

NASA TM X-71457

CALCULATION PROCEDURES FOR POTENTIAL AND VISCOUS FLOW SOLUTIONS FOR ENGINE INLETS

by J. A. Albers and N. O. Stockman
Lewis Research Center
Cleveland, Ohio

TECHNICAL PAPER proposed for presentation at 1974 International Gas Turbine Conference sponsored by the American Society of Mechanical Engineers Zurick, Switzerland, March 31-April 4, 1974

CALCULATION PROCEDURES FOR POTENTIAL AND VISCOUS FLOW SOLUTIONS FOR ENGINE INLETS

by

J. A. Albers* and N. O. Stockman+

Lewis Research Center
National Aeronautics and Space Administration
Cleveland, Ohio

ABSTRACT

The method and basic elements of computer solutions for both potential flow and viscous flow calculations for engine inlets are described. The procedure is applicable to subsonic conventional (CTOL), short-haul (STOL), and vertical takeoff (VTOL) aircraft engine nacelles operating in a compressible viscous flow. The calculated results compare well with measured surface pressure distributions for a number of model inlets. The paper discusses the uses of the program in both the design and analysis of engine inlets, with several examples given for VTOL lift fans, acoustic splitters, and for STOL engine nacelles. Several test support applications are also given.

---

*Aerospace Research Engineer, V/STOL Propulsion Technology Branch, Member ASME

+Aerospace Research Engineer, V/STOL Propulsion Technology Branch

INTRODUCTION

One of the significant areas in propulsion technology for advanced subsonic conventional (CTOL), short-haul (STOL), and vertical takeoff (VTOL) aircraft is the design of the engine inlet section. For these high performance aircraft, the engine inlets are required to operate efficiently over wide ranges of mass flow, flight speed, and incidence angle. Furthermore, some applications may require unique configurations or considerations such as sound absorbing splitter rings, contouring for high-velocity throat section, low rotor inlet distortion, etc. Because of the great importance of efficient inlet flow on both engine performance and noise radiation during takeoff and landing, considerable research and development effort is required for the design of high-performance inlets.

The principal tool in inlet design has been wind tunnel experiments with scaled models of inlets. This approach is an expensive and complex pursuit because of the very large number of geometric and flow variables involved. An extremely valuable asset in inlet design would be a computer program for the calculation of the potential and viscous flow within the inlet for a wide range of aircraft applications, inlet configurations, and operating conditions. Such a calculation procedure would provide a valuable tool for: (1) parametric studies of the effect of inlet design variables and configurations; (2) analysis and correlation of test data; and (3) formulation of more efficient and economical test programs.

The NASA Lewis Research Center is in the process of developing computer programs for the calculation of potential and viscous flows in engine inlets. The original application for the program was the design of inlets for VTOL lift fans (refs. 1 and 2). The effort has now been extended to calculation procedures for inlets for conventional and short-haul engine nacelles (refs. 3, 4, 5, 6, and 7) with provision for the incorporation of additional bodies such as acoustic splitter rings.

The computer program system contains a number of basic elements. The chief element is the Douglas program for incompressible potential flow (ref. 8). A program was written (ref. 9) to represent the inlet geometry by analytical contours for input to the Douglas program. Another program was written (ref. 9) to combine basic incompressible potential flow solutions to produce a solution for any combination of mass flow, free-stream velocity, and angle of attack. The combination program incorporates a compressibility correction (ref. 10) that can handle local transonic Mach numbers. The viscous flow solution is based on the Princeton method for calculating compressible boundary layers on curved surfaces (ref. 11), with routines added to calculate boundary layer transition (ref. 12).

This paper presents a status report on the development and applications of the above-mentioned computer effort. The basic elements and procedures of the computer solutions for both the potential flow and viscous flow calculations are first described. Examples are given of the comparison between calculated and measured surface pressure distributions

for a number of model inlets. The paper then discusses the uses of the program in both the design and analysis of engine inlets, with several examples given for specific cases involving inlets for VTOL lift fans and for short-haul engine nacelles. Finally the use of the method as a test support tool is discussed.

NOMENCLATURE

A,B,C,	combination coefficients
Δi	change in rotor incidence angle between static and cross-flow operation
C_f	skin friction coefficient
H	shape factor, δ^*/θ
L	distance from inlet highlight to diffuser exit
M	Mach number
$\overline{M}_c$	average axial Mach number at fan face
N	normal to the body surface
P_t	total pressure
p	static pressure
q	dynamic pressure
p,t	arbitrary points on the surface of the inlet
R	distance between two surface points
r	radius from centerline
S_A	surface area
S	local surface distance from stagnation point

S_{max}	total surface distance from stagnation point to diffuser exit
U_T	rotor tip speed
u	axial velocity in boundary layer
V	potential flow velocity
$\overline{V}_c$	average axial velocity at control station
V_{cr}	critical velocity (local speed at Mach one)
X	distance from inlet highlight
α	incidence angle at inlet, direction of free-stream velocity relative to inlet axis
δ	boundary layer thickness
δ^*	displacement thickness
θ	momentum thickness
μ	molecular viscosity
ρ	density
σ	surface source strength per unit area
τ	shear stress

Superscript

$\overline{\quad}$	average value across inlet flow passage
$\vec{\quad}$	vector

Subscript

i	incompressible
ref	reference
T	tip
w	wall
∞	free-stream at inlet, usually taken equal to undisturbed free-stream

0	parallel to inlet axis
1,2,3	referes to basic potential flow solutions
90	perpendicular to inlet axis

CALCULATION PROCEDURE

The calculation procedure developed for the analysis and design of engine inlets operating in a compressible viscous flow field is discussed in the following order: 1) geometry definition, 2) incompressible potential flow, 3) compressibility, 4) viscous flow, and 5) overall program.

Geometry Definition

Potential flow calculation procedures are quite sensitive to geometry in that they require geometric coordinates and point spacing to be distributed properly for accurate solutions on the inlet surfaces. A program denoted SCIRCL was developed to generate accurate input coordinates for a prescribed inlet geometry. Representative inlet geometries for potential flow solutions are shown in figure 1(a) for a conventional inlet and in figure 1(b) for a VTOL inlet. For both inlet geometries the duct extension is an artifice to permit specification of mass flow through the inlet.

For the VTOL inlet (fig. 1(b)) the two-demensional pod or wing section is replaced by the artificial bellmouth extension which now represents an axisymmetric surface. This artifice facilitates the use of the axisymmetric potential flow program for VTOL configurations.

The actual geometry is prepared for input to SCIRCL by dividing the inlet surfaces and extensions into segments each of which is a portion of an analytical curve as illustrated in figure 2. The curves available are

straight lines, cubics, superellipses*, ellipses, and lemniscates. SCIRCL distributes points along the inlet surfaces in such a way as to meet the requirements of the potential flow program. SCIRCL outputs printed information about the inlet surfaces such as, coordinates, curvature, slope, etc. In addition to the surface points, SCIRCL generates points spanning the inlet passage (like flow measuring rakes) at axial locations where velocity profiles or streamlines are desired.

Incompressible Potential Flow

The Douglas Neumann program is used for calculating the incompressible potential flow field (ref. 8). The program utilizes a large number of sources and sinks of initially unknown strengths on the surface of the inlet. It is assumed that each surface element is a straight line segment and that the source or sink is located at the midpoint of each element. The central problem of the Douglas analysis is the solution of the integral equation

$$2\pi\sigma(p) - \int_{S_A} \frac{\partial}{\partial N}\left[\frac{1}{R(p,t)}\right] \sigma(t)\, dS_A = -\vec{V}_\infty \cdot \vec{N} \qquad (1)$$

where σ is the unknown source strength on each surface element. The first term of equation (1) is the normal velocity induced at p (an arbitrary point on the inlet surface), by a source at p. The second

*a superellipse has the form

$$\left(\frac{x}{a}\right)^n + \left(\frac{y}{b}\right)^n = 1.0$$

term is the combined effect of the sources at other points t on the surface of the inlet. The quantity $\frac{\partial}{\partial N}\left[\frac{1}{R(p,t)}\right]$ depends only on the geometry of the surface. The term on the right of equation (1) is the normal component of the free-stream velocity at p. The above integral equation is approximated by a set of linear algebraic equations and then solved by matrix methods. The velocities on and off the body surface are calculated from the source distribution.

The Douglas axisymmetric potential flow program, denoted EOD, is used to obtain three basic solutions for flow about inlets. These solutions (see fig. 3) are: $\vec{V}_1$, axial flow with inlet duct extension closed; $\vec{V}_2$, axial flow with the duct open, and $\vec{V}_3$, the crossflow solution with the duct extension open.

A third computer program denoted COMBYN combines the three basic solutions into a solution of interest that can be expressed as

$$\vec{V} = A\vec{V}_1 + B\vec{V}_2 + C\vec{V}_3 \qquad (2)$$

The combination coefficients A, B, and C are determined by specifying any combination of 1) free-stream velocity V_∞, 2) inlet incidence angle α, and 3) average axial velocity $\bar{V}_c$ (or mass flow rate) as specified at a control station in the inlet (fig. 4). The control station is a "rake" of off-body points in the inlet.

Compressibility

The program COMBYN corrects the incompressible potential flow solution for compressibility using the method of reference 10. The compressibility correction for internal flow solutions was proposed in reference 10, as

$$V = V_i \left(\frac{\rho_i}{\bar{\rho}} \right)^{V_i/\bar{V}_i} \tag{3}$$

where

V the local compressible velocity

V_i the local incompressible velocity

$\bar{V}_i$ the average incompressible velocity across the flow passage

ρ_i incompressible density (equal to the compressible stagnation density)

$\bar{\rho}$ average compressible density across flow passage

This expression was developed by comparing exact compressible and incompressible solutions for flow through a turbine blade passage. However, the correction has been shown to be applicable to engine nacelle inlets (ref. 5).

Equation (3) was derived for internal flow solutions and cannot be applied directly to external inlet surfaces because there is no flow passage in which the average velocity $\bar{V}_i$ can be calculated. In order to apply equation (3) to external flows, an artificial value of $\bar{V}_i$ is

specified. For the static case ($V_\infty = 0$), $\bar{V}_i$ can be based on some arbitrary area representative of the average external flow. For the non-zero V_∞ case, $\bar{V}_i$ is set equal to V_∞ and equation (3) becomes

$$V = V_i \left(\frac{\rho_i}{\rho_\infty} \right)^{V_i/V_\infty} \tag{4}$$

where ρ_∞ is the free stream static density. This simple expression compares favorably with the Goethert compressibility correction (ref. 13).

Viscous Flow

The surface Mach number distributions obtained from the program COMBYN are used as an input to program VISCUS which calculates the boundary layer growth and separation point (if any) on the inlet surface. Program VISCUS is a modified version of the Herring and Mellor boundary layer program (ref. 11) which solves the partial differential equations of mass, momentum, and energy. This method linearizes the partial differential equations by using finite differences for the x derivatives resulting in a series of ordinary differential equations. The ordinary differential equations are then integrated numerically across the boundary layer at each x-location. Mellor and Herring, in formulating their effective viscosity hypothesis, divide the boundary layer in terms of an inner layer and outer layer and an overlap layer. The viscosity of each region is based on experimental data and is uniquely determined by values

of a pressure gradient parameter and displacement thickness Reynolds number (refs. 14 and 15). The effective viscosity hypothesis as used in the program includes the influence of longitudinal wall curvature (ref. 16). The boundary layer calculations start at the stagnation point on the inlet. The Falkner-Skan laminar wedge flow solution (ref. 17) for stagnation point flow was used for a starting profile.

The prediction of boundary layer transition is a necessary part of any viscous flow analysis. In the Herring and Mellor program the location of the transition point was a program input. However, internal means to effect transition were included in program VISCUS (ref. 12). The transition region is defined as the region between the instability point (or critical point) and the fully turbulent point. The physical factors which influence the transition region that have been accounted for include pressure gradient, surface roughness, free stream turbulence level, and longitudinal curvature. The empirical correlations for these factors were obtained from reference 17.

It is important that the development of the laminar and turbulent boundary layer be accurately determined to ascertain whether the boundary layer would separate and, if so, at what point on the inlet surface. The criterion used to determine the point of separation is the condition of zero wall shear stress (zero skin friction coefficient).

Overall Program

The four computer programs discussed previously can be combined into a single program as illustrated in figure 5. The overall calculation

procedure consists of the following components: 1) geometry definition (SCIRCL) for input into the potential flow program; 2) calculation of basic incompressible potential flow (EOD); 3) combination of the basic incompressible potential flow solutions and correction for compressibility (COMBYN); 4) calculation of the viscous flow characteristics based on the results of the potential flow (VISCUS): 5) redefinition of inlet geometry by addition of boundary-layer displacement thickness; 6) recalculation of potential flow and viscous flow solution; and 7) iteration of the above scheme until convergence is achieved. It is contemplated that the four main segments of the program system (SCIRCL, EOD, COMBYN, and VISCUS) be combined to run under the control of a main routine. At present, program SCIRCL and EOD are run independently with punched output from one segment being fed into the next segment. However, programs COMBYN and VISCUS have been successfully mated and have been run for a variety of input conditions.

COMPARISONS WITH EXPERIMENT

To establish the validity of the calculation procedure comparisons were made with experimental data for 1) VTOL inlets, 2) translating centerbody inlet in both a choked and unchoked mode, and 3) an inlet operating at cruise conditions. All the experimental data except figure 6 were obtained at the NASA Lewis Research Center. The data of figure 6 were obtained from the National Research Council of Canada (ref. 18).

VTOL Inlets

Comparisons between experiment and theory are given for both fan-in-wing and fan-in-pod configurations. The surface pressure distribution in a chordwise cut of a fan-in-wing inlet is shown in figure 6. Three surfaces are shown in the plot, and the distance on the abscissa corresponds to the numbers indicated on each surface in the inset: the forward surface of the bellmouth, the surface of the centerbody, and the aft surface of the bellmouth. The agreement is quite good everywhere on the inlet. It should be noted that the Mach number of this test was very low (0.2) so that compressibility was not a factor. However, this case was presented to illustrate the applicability of the method when the actual geometry differs from the artificial geometry (see fig. 1(b)).

The next case illustrates the applicability of the method when the flow is compressible. Figure 7 shows the theoretical and experimental surface pressure distributions on a fan-in-pod inlet (described in ref. 19). Both incompressible and incompressible corrected for compressibility theoretical curves are given. The experimental static pressures agree quite well with the theory corrected for compressibility along the entire surface of the inlet.

Translating Centerbody Inlet

Unchoked mode. - A translating centerbody inlet with the centerbody retracted is shown in figure 8(a). The configuration is a conventional subsonic inlet with an NACA series one external cowl shape and a two-to-

one ellipse internal lip. The contraction ratio (highlight area/throat area is 1.30 and the diameter at the diffuser exit is 13.97 centimeters.

A comparison with data and theory is shown in figure 8(b) for static conditions. Three theoretical curves are shown: (1) the incompressible potential flow solution; (2) the incompressible solution corrected for compressibility; and (3) the corrected solution with boundary layer displacement thickness taken into account. The incompressible potential flow solution with the compressibility correction compared well with the experimental data in the first half of the inlet. In the aft portion of the diffuser the theoretical static pressures were on the average 2 percent higher than experimental data. However, when both the compressibility correction and boundary layer displacement thickness were included, the theoretical and experimental static pressures were in good agreement over the entire length of the diffuser.

A comparison between theory and experiment at high inlet incidence angle (40°) with forward velocity is illustrated in figure 8(c). Engine inlets of short haul aircraft will be exposed to larger incidence angles than inlets of conventional aircraft (ref. 20) because of the high lift coefficients and low speeds necessary for takeoff and landing operations. Good agreement was found between experimental data and theory except at the inlet highlight ($X/L = 0$) where the theoretical static pressures were lower than experimental data. The boundary-layer correction was effective in improving the solution at incidence angle in spite of the fact the boundary layer is not uniformly distributed circumferentially in the aft portion of the diffuser.

Choked mode. - The translating centerbody inlet with the centerbody extended is shown in figure 9. This illustrates an inlet operating in the takeoff choked mode with the centerbody extended forward of the inlet highlight producing a reduced throat area. Internal surface static pressure distributions are shown for a free-stream velocity of 32 m/sec and at inlet incidence angles of 20 and 40 degrees. Reasonable comparison between data and theory was obtained. The slight difference between the data and theory in the aft portion of the diffuser ($X/L > 0.6$) can be attributed to neglecting the boundary layer displacement thickness in the potential flow solution.

Inlet at Cruise Conditions

To illustrate the applicability of the method at high free-stream Mach numbers a comparison of calculated internal surface static pressures (without boundary layer correction) with experimental data on an inlet operating at a cruise free-stream Mach number of 0.75 is shown in figure 10. The inlet geometry is a conventional subsonic inlet with an NACA series one external cowl shape and a two-to-one ellipse internal lip with contraction ratio of 1.26. In general, good agreement between theoretical and experimental static pressures was obtained over the entire length of the inlet lip and diffuser.

APPLICATIONS

The capability of the method in adequately predicting the real flow in various inlets as shown in the previous section makes it extremely

useful for several applications. Examples to be given include VTOL inlet design, STOL inlet design, acoustic splitter design, boundary layer characteristics, and test support.

VTOL Inlet Design

An example of the use of surface velocity distributions and passage velocity profiles in the design of a VTOL fan-in-pod inlet is shown in figure 11. The specific problem in this case is the determination of a near optimum location of the point of tangency between the bellmouth and the pod surface. Three locations of this tangent point are shown in the inset in figure 11(a). The theoretical surface velocity distributions on the three different bellmouths are also shown for both static and crossflow operation. It can be seen that both the velocity peaks and the unfavorable velocity gradients in crossflow are reduced as the tangent point is moved out to a larger radius, thus case C would be expected to have the best crossflow performance. However, at static conditions case C shows a higher velocity peak and a more adverse velocity gradient than cases A and B. In order to select a best shape a compromise may be made between the static and crossflow operation.

The radial velocity profiles at the fan face are shown in figure 11(b) for both static and crossflow conditions. The differences between the three cases were not significant enough to affect the choice. However another application of the method can be pointed out here, namely that the calculated static velocity profile as well as the upstream streamlines can be used as input to the fan rotor design.

A further example of VTOL inlet calculations is given in figure 12, which illustrates the effect of crossflow on the potential flow rotor incidence angle for the fan-in-wing inlet shown in the figure. The rotor of the fan and the inlet were both designed for static operation with a ratio of tip speed to fan axial velocity of 1.67. If this inlet is operated at a ratio of crossflow velocity to fan axial velocity of around 0.4, the incidence angle of the potential flow relative to the rotor blades will deviate from the design value by magnitude Δi, as indicated by the contours in figure 12. It can be seen that, in the plane of the rotor inlet, the incidence angle distortion due to the potential flow alone can be severe. (Incidence angle distortion does not include inlet total pressure variations or the modification of the potential flow due to the presence of the rotor.) Similar results can be obtained to study the effect of different design parameters such as inlet depth, transition velocity, inlet profile, and rotor conditions.

Short-Haul Inlet Design

An example of application to short-haul inlet design is shown in figure 13. Internal lip geometries are shown in figure 13(a) for inlet contraction ratios ranging from 1.3 to 1.42. The surface Mach number distributions are presented in figure 13(a) and the Mach number profiles at the throat location are shown in figure 13(b). The surface Mach numbers are plotted versus fractional surface distance from the stagnation point on the inlet to a reference plane in the inlet duct. This figure indicates a large effect of inlet lip geometry on sur-

face Mach number levels and gradients, but a relatively small effect on the velocity profiles. Mach number distributions such as these can aid a designer in selecting an inlet geometry for a given application.

Acoustic Splitter Design

An application of the prediction method to acoustic splitter location and design is shown in figure 14. The method is used to obtain the cruise streamline along which the splitter is to be aligned (fig. 14(a)). After a preliminary design of the splitter, surface Mach number distributions on the splitter surface (fig. 14(b)) were obtained at cruise and takeoff conditions to aid in achieving a compromise between aerodynamic and acoustic requirements of the splitter. Examination of the Mach number distributions shows that similar Mach number gradients were obtained on both the inner and outer surfaces. This similarity is indicative of a properly aligned splitter. The potential flow solution can also be used to optimize the shape of the splitters by minimizing Mach number gradients for various splitter goemetries.

Boundary Layer Characteristics

The calculation procedure provides boundary-layer results for determining if separation will occur. An example, illustrating the boundary layer characteristics for the nacelle inlet of figure 10, for an attached flow condition is shown in figure 15. The boundary layer parameters presented are: the shape factor H, the skin friction coefficient C_f, and

boundary layer velocity profiles. Also shown is the predicted location of the transition region. The skin friction coefficient decreases sharply in the laminar portion of the flow but separation is not indicated. The velocity profiles in the boundary layer at various locations along the surfaces are typical laminar and turbulent profiles.

An example illustrating the boundary layer characteristics for a separated flow condition for the inlet at 50° incidence angle is shown in figure 16. Also shown are theoretical and experimental separation locations. The skin friction coefficient decreases sharply to zero in the laminar portion of the flow due to the large adverse Mach number gradient. Good agreement was obtained between experimental and theoretical separation locations.

Test Support

The theoretical inlet calculations can be useful in analyzing and understanding experimental results. The calculations have been used for test support in several experimental programs conducted at the Lewis Research Center.

The most widespread application in test support has been in the calibration of test inlets for mass flow determination. The computer program is used to generate a correlation of integrated mass flow with static pressure at some location on the test inlet surface. This correlation and the measured static pressure are then used to determine the mass flow through the test inlet. This type of mass flow calibration has been successfully used in tests reported in references 19, 21, 22, and 23.

The method also provides surface pressure distributions for calculation of inlet surface forces. Inlet additive drag is frequently calculated from the mass flow rate and the location of the stagnation point which is difficult to determine experimentally. With the inlet programs additive drag may be determined by integrating static pressures on the inlet capture stream tube. Inlet cowl suction force can be determined by integrating the cowl surface static pressure from the stagnation point to the location of maximum nacelle diameter. The inlet net force can be obtained from the additive drag and the cowl suction force.

In addition, the calculation procedure can be used to determine surface pressures and forces on boattails. For some engine nacelles the cowl pressure distribution may be influenced by the flow over the aft end of the nacelle due to the relative proximity of the inlet and boattail. The method could be used to investigate the interaction between the inlet and boattail for a given experimental configuration.

Theoretical circumferential variations of flow parameters at the fan face can also be used in test support. In reference 21 the theoretical change in rotor incidence angle was used as an aid in interpreting the variation in rotor exit total pressure ratio observed in the test. Also the theoretical distribution of rotor inlet flow angle was used to interpret the experimental distribution of rotor outlet flow angle.

CONCLUDING REMARKS

A theoretical method based on incompressible potential flow corrected for compressibility and boundary layer in axisymmetric inlets was described.

Several sample calculations and comparisons with experiments were presented which demonstrated the reliability of the method, and further applications were illustrated. The method should be a very useful and powerful tool in both the design and analysis of various types of high-performance inlets for propulsion systems.

REFERENCES

1. Stockman, N. O., and Lieblein, S., "Theoretical Analysis of Flow in VTOL Lift Fan Inlets Without Crossflow," TN D-5065, 1969, NASA, Cleveland, Ohio.

2. Stockman, N. O., "Potential Flow Solutions for Inlets of VTOL Lift Fans and Engines," Analytic Methods in Aircraft Aerodynamics, SP-228, 1970, NASA, Washington, D. C., pp. 659-681.

3. Albers, J. A., "Theoretical and Experimental Internal Flow Characteristics of a 13.97-Centimeter Diameter Inlet at STOL Takeoff and Approach Condition," TN D-7185, 1973, NASA, Cleveland, Ohio.

4. Albers, J. A., and Miller, B. A. "Effect of Subsonic Inlet Lip Geometry on Predicted Surface and Flow Mach Number Distributions," TN D-7446, 1973, NASA, Cleveland, Ohio.

5. Albers, J. A., "Application of Compressibility Correction to Calculation of Flow in Inlets," Journal of Aircraft, Vol. 10, No.7, July 1973, pp. 441-442.

6. Albers, J. A., "Comparison of Predicted and Measured Low Speed Performance of Two 51 Centimeter Diameter Inlets at Incidence Angle," NASA TM X-2937, 1973, NASA, Cleveland, Ohio.

7. Albers, J. A., and Felderman E. J., ''Boundary Layer Analysis of Subsonic Inlet Diffuser Geometries,'' proposed Technical Note, 1973, NASA, Cleveland, Ohio.

8. Hess, J. L., and Smith, A. M. O., ''Calculation of Potential Flow About Arbitrary Bodies, Progress in Aeronautical Sciences, Vol. 8, O. Küchemann, ed., Pergamon Press, 1967, pp. 1-138.

9. Stockman, N. O., and Button, S. L., ''Computer Programs for Calculating Potential Flow in Propulsion System Inlets,'' TM X-68278, 1973, NASA, Cleveland, Ohio.

10. Lieblein, S., and Stockman, N. O., ''Compressibility Correction for Internal Flow Solutions,'' Journal of Aircraft, Vol. 9, No. 4, Apr. 1972, pp. 312-313.

11. Herring, H. J., and Mellor, G. L., ''Computer Program for Calculating Laminar and Turbulent Boundary Layer Development in Compressible Flow,'' CR-2068, 1972, NASA, Washington, D. C.

12. Albers, J. A., and Gregg, J. L., ''A Computer Program to Calculate Laminar, Transitional, and Turbulent Boundary Layers for Compressible Axisymmetric Flow,'' proposed Technical Note, 1973, NASA, Cleveland, Ohio.

13. Shapiro, A. H., The Dynamics and Thermodynamics of Compressible Fluid Flow, Vol. I, Ronald Press, 1953, pp. 316-321.

14. Mellor, G. L., and Gibson, D. M., ''Equilibrium Turbulent Boundary Layers,'' Journal of Fluid Mechanies, Vol. 24, Pt. 1, 1966, pp. 225-253.

15. Mellor, G. L., "The Effects of Pressure Gradients on Turbulent Flow Near a Smooth Wall," Journal of Fluid Mechanies, Vol. 24, Pt. 2, 1966, pp. 254-274.

16. So, R. M. C., and Mellor, G. L., "An Experimental Investigation of Turbulent Boundary Layers Along Curved Surfaces," CR-1940, 1972, NASA, Washington, D. C.

17. Schlichting, H. (J. Kestin, trans.), Boundary Layer Theory, Sixth ed., McGraw-Hill Book Co., pp. 431-516.

18. Schaub, U. W., "Experimental Investigation of Flow Distortion in Fan-in-Wing Inlets," Journal of Aircraft, Vol. 5, No. 5, Sept.-Oct. 1968, pp. 473-478.

19. Stockman, N. O., Loeffler, I. J., and Lieblein, S., "Effect of Rotor Design Tip Speed on Aerodynamic Performance of a Model VTOL Lift Fan Under Static and Crossflow Condition," Journal of Engineering for Power, Vol. 95, No. 4, Oct. 1973, pp. 293-300.

20. Albers, J. A., "Predicted Upwash Angles at Engine Inlets for STOL Aircraft," TM X-2593, 1972, NASA, Cleveland, Ohio.

21. Lieblein, S., Yuska, J. A., and Diedrich, J. D., "Performance Characteristics of a Model VTOL Lift Fan in Crossflow, Journal of Aircraft, Vol. 10, No. 3, Mar. 1973, pp. 131-136.

22. Miller, B. A., and Abbott, J. M., "Low-Speed Wind-Tunnel Investigation of the Aerodynamic and Acoustic Performance of a Translating-Centerbody Choked-Flow Inlet," TM X-2773, NASA, Cleveland, Ohio.

23. Wesoky, H. L., and Steffen F. W., ''Wind Tunnel Tests of a 20 Inch Diameter 1.15 Pressure Ratio Fan Engine Model,'' Paper No. 73-1216, 1973, AIAA, New York.

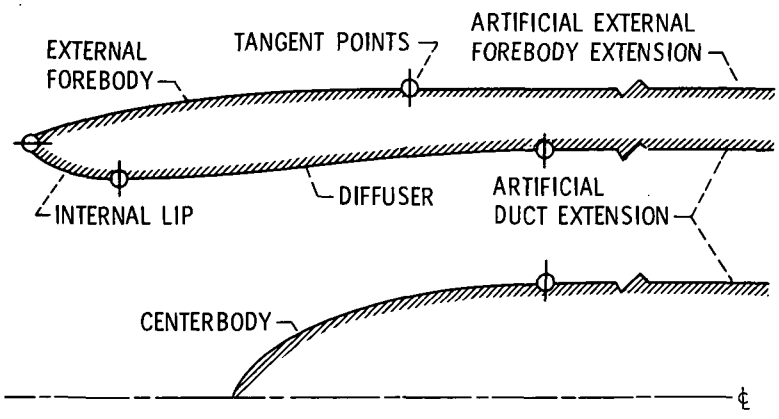

(a) CONVENTIONAL INLET.

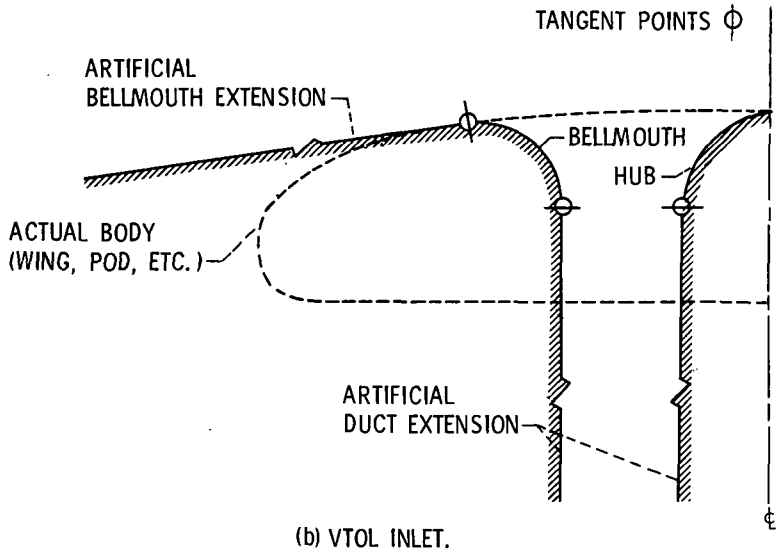

(b) VTOL INLET.

Figure 1. - Representative inlet geometries for potential flow solutions.

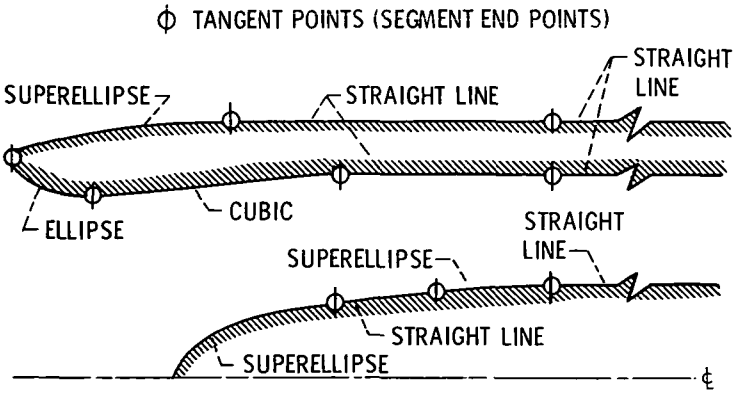

Figure 2. - Typical segmentation of inlet profile.

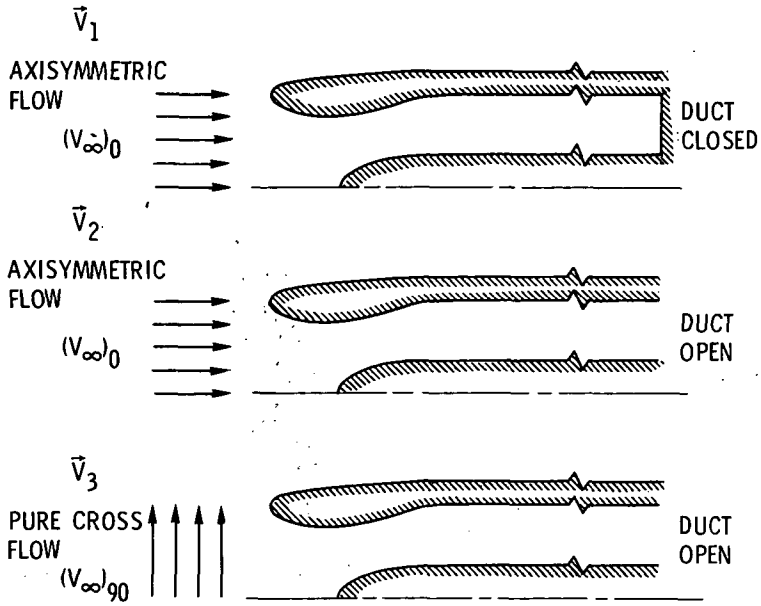

Figure 3. - Flow conditions and inlet geometry for basic solutions.

$\bar{V}_c$ AVERAGE AXIAL VELOCITY AT CONTROL STATION
V_∞ MAGNITUDE OF FREE-STREAM VELOCITY AT INLET
α DIRECTION OF FREE-STREAM VELOCITY AT INLET

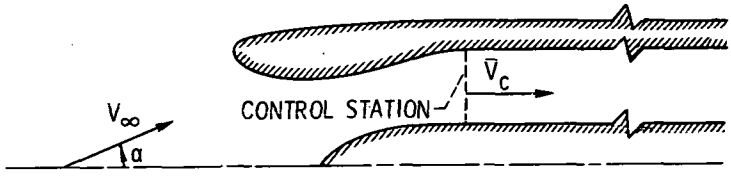

Figure 4. - Flow conditions for combined solution.

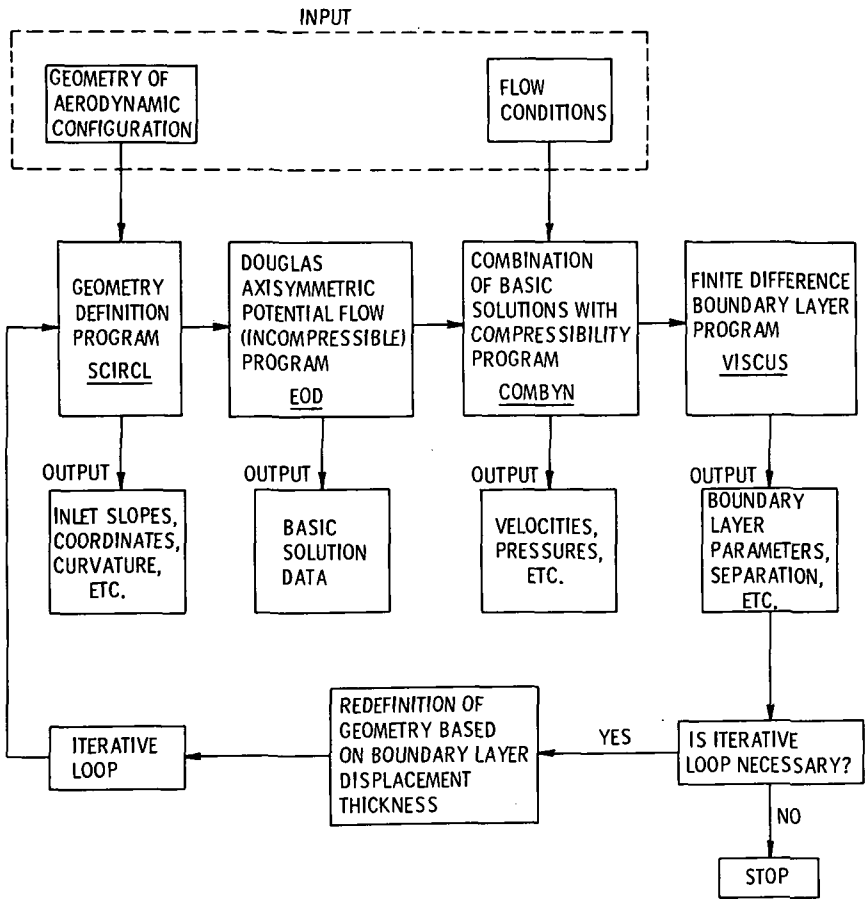

Figure 5. - Schematic of overall program for inlets.

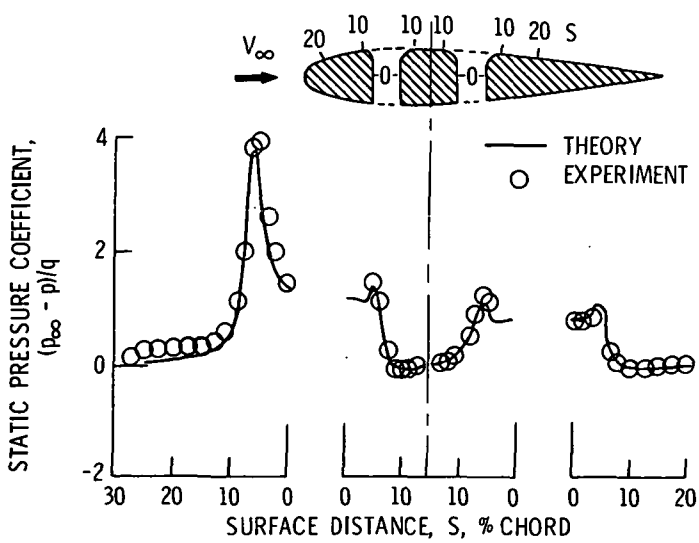

Figure 6. - Comparison with experiment of fan-in-wing surface pressure distribution. Average rotor inlet Mach number, $\bar{M}_c = 0.19$, $V_\infty/\bar{V}_c = 0.27$.

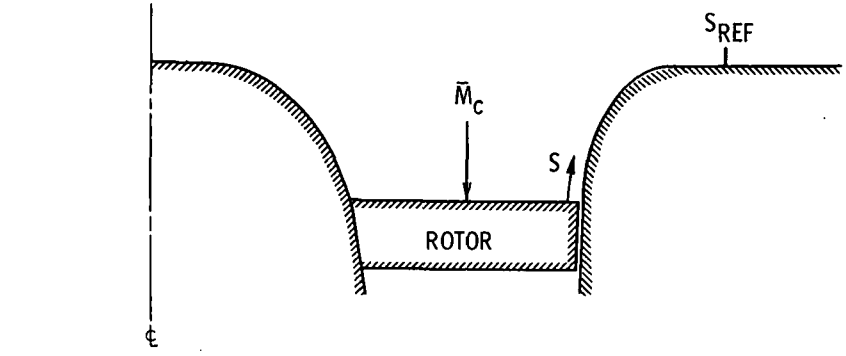

Figure 7. - Comparison with experiment of fan-in-pod inlet surface pressure distribution. Static condition, $V_\infty/\bar{V}_C = 0$. Average rotor inlet Mach number, $\bar{M}_C = 0.57$.

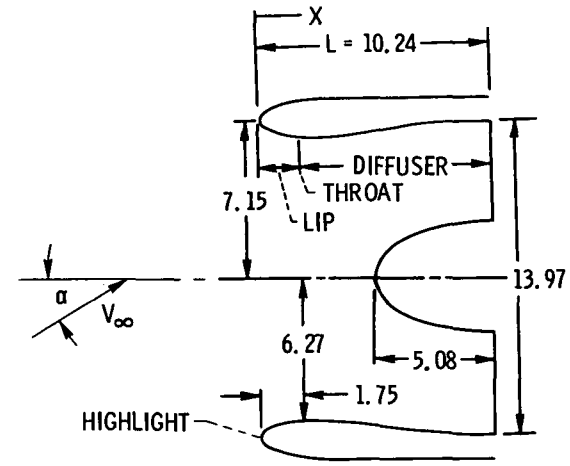

(a) INLET GEOMETRY. (ALL DIMENSIONS IN CM.)

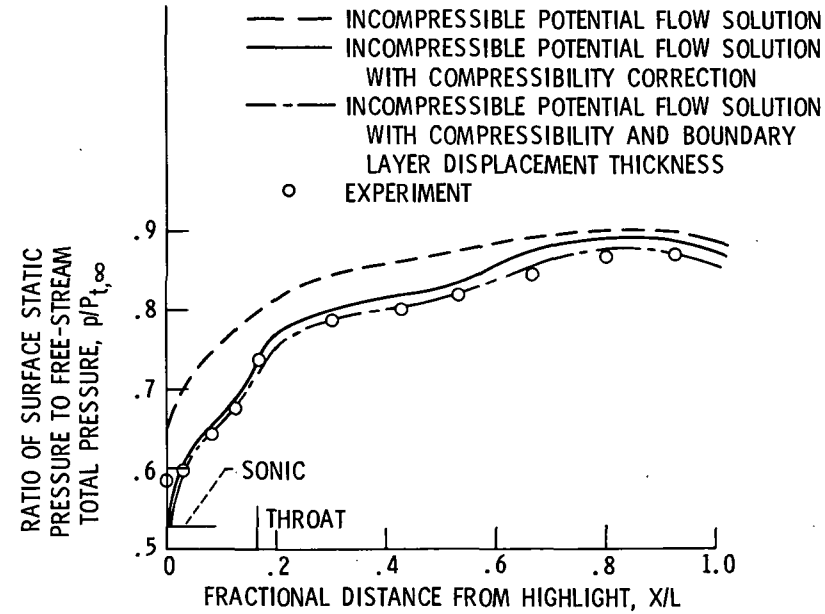

(b) STATIC CONDITION.

Figure 8. - Comparison with experiment of internal surface pressure distributions for translating centerbody inlet in the unchoked mode.

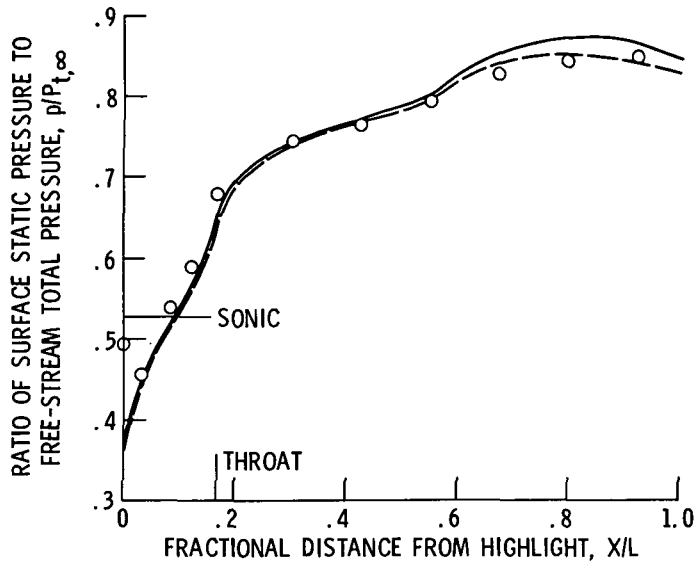

(c) FREE-STREAM VELOCITY, V_∞, 24 METERS PER SECOND; INCIDENCE ANGLE, α, 40^0; WINDWARD SIDE OF INLET.

Figure 8. - Concluded.

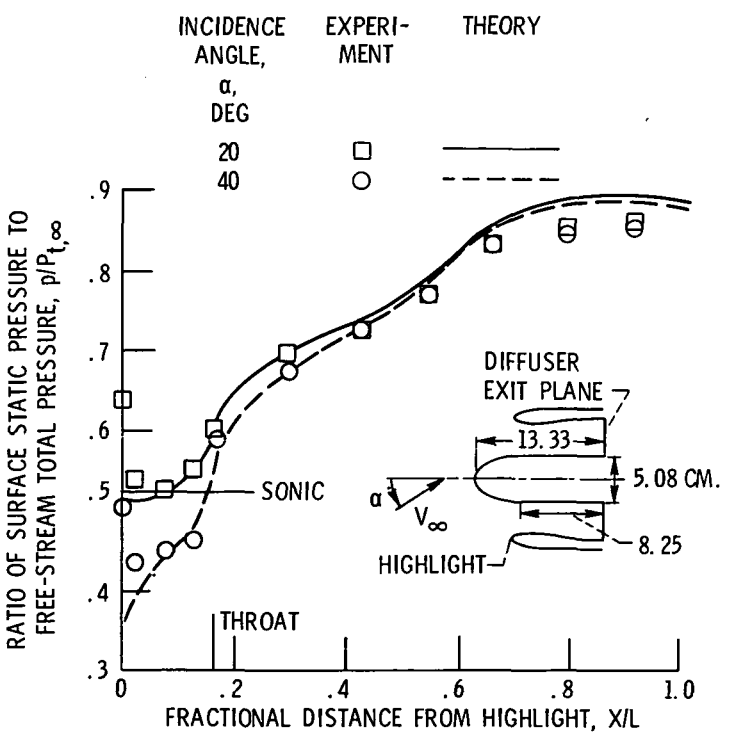

Figure 9. - Comparison with experiment of internal surface pressure distribution for translating centerbody inlet in the choked mode. Free-stream velocity, V_∞, 32 m/sec; windward side of inlet.

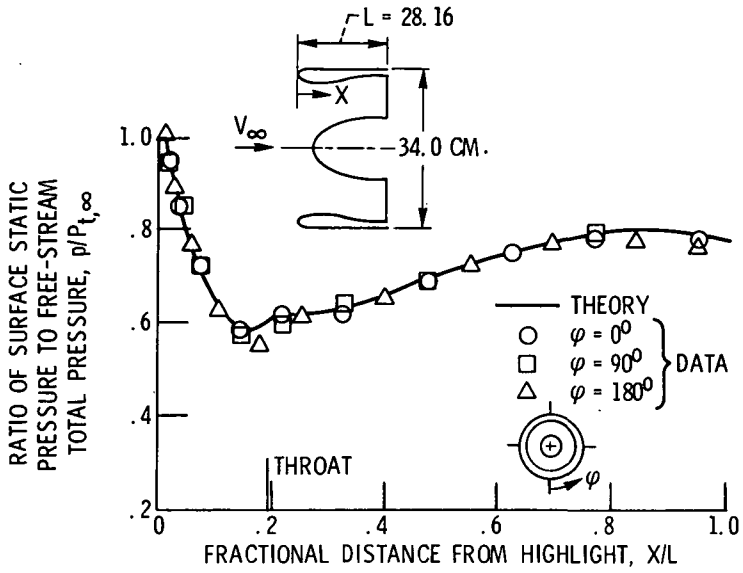

Figure 10. - Comparison with experiment of internal surface pressure distribution for inlet at cruise. Free-stream Mach number, M_∞, 0.75; incidence angle, α, 0^0; inlet mass flow ratio, 0.66.

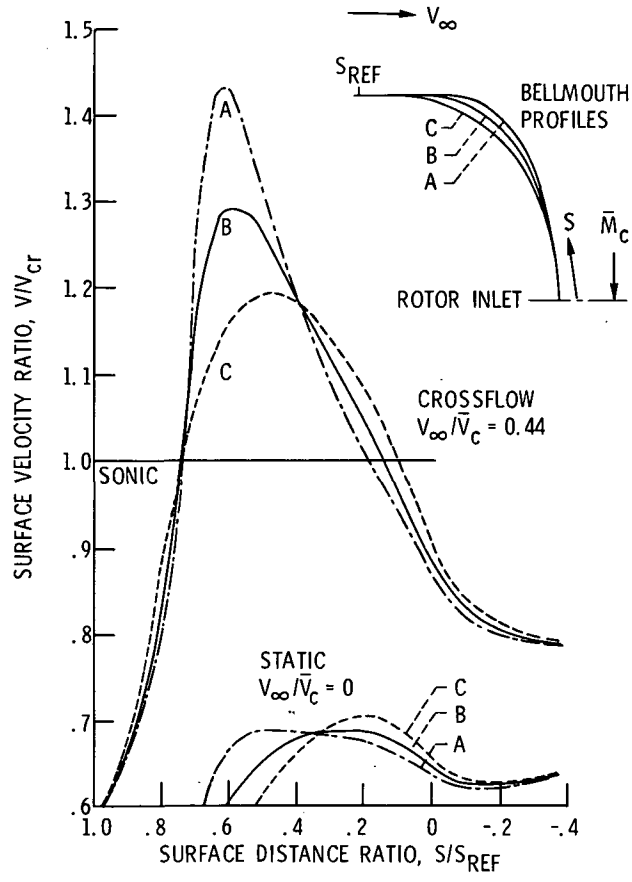

(a) SURFACE VELOCITY DISTRIBUTION.

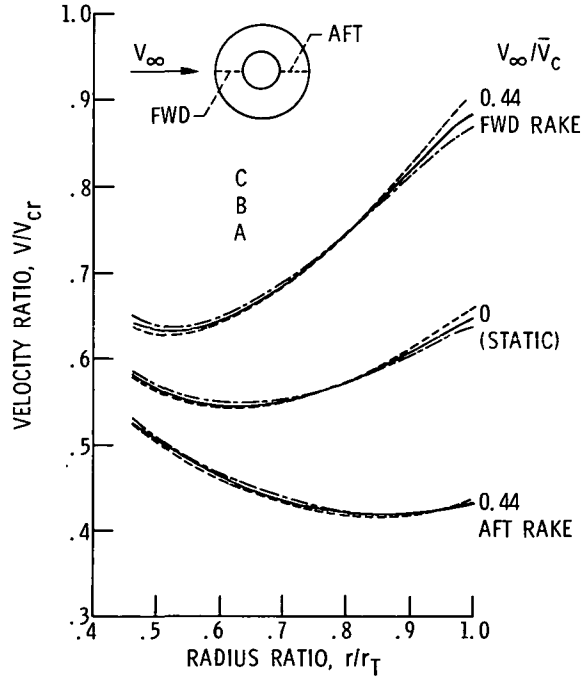

(b) FAN FACE VELOCITY PROFILES.

Figure 11. - Application of theory to VTOL inlet design. Average rotor inlet Mach number, $\bar{M}_c = 0.53$.

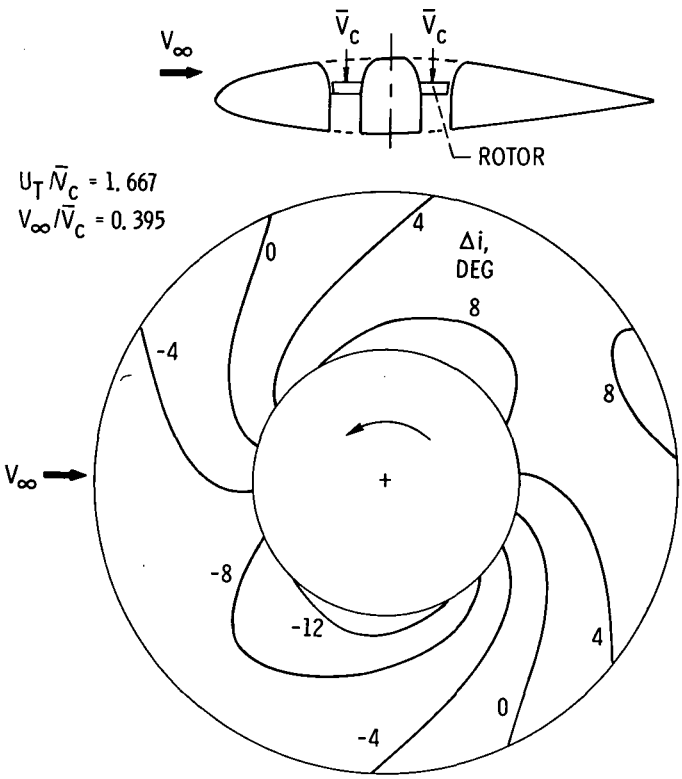

Figure 12. - Application of theory to VTOL rotor inflow distortion in crossflow.

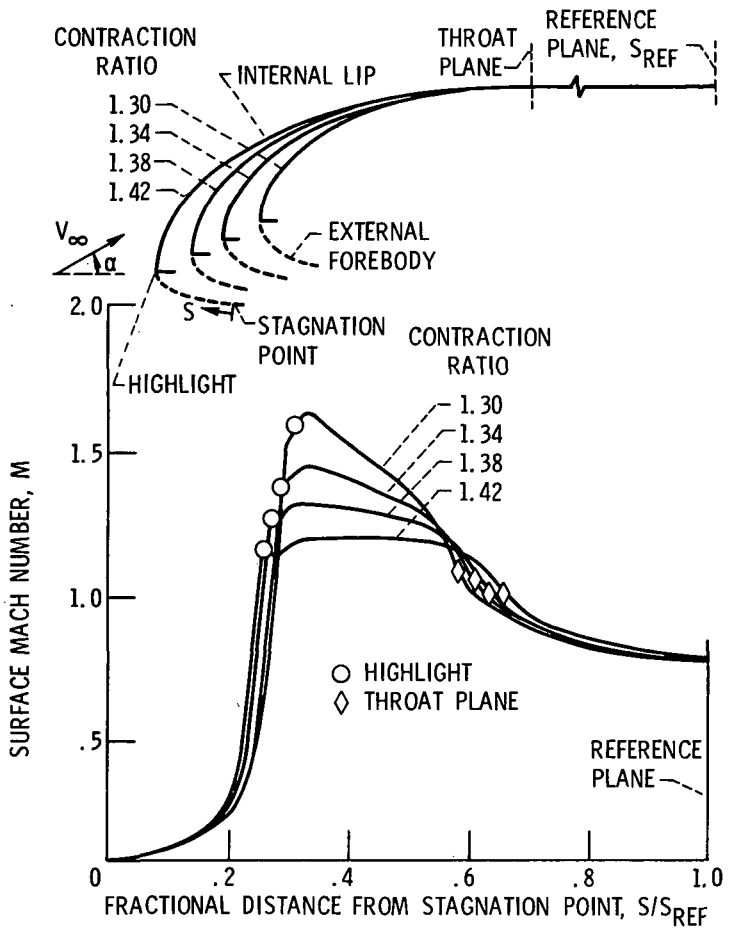

(a) SURFACE MACH NUMBER DISTRIBUTION.

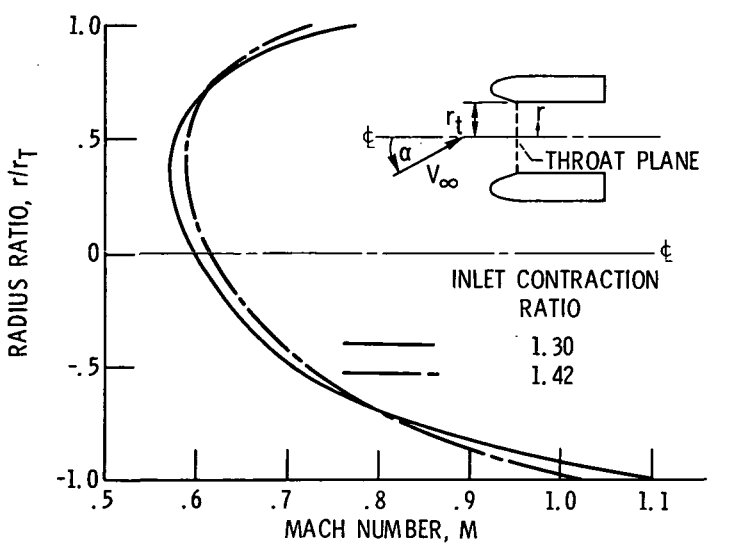

(b) MACH NUMBER PROFILE AT THROAT PLANE.

Figure 13. - Application of theory to short-haul inlet design. Free-stream velocity, V_∞ = 42.6 m/sec, incidence angle, $\alpha = 30^0$.

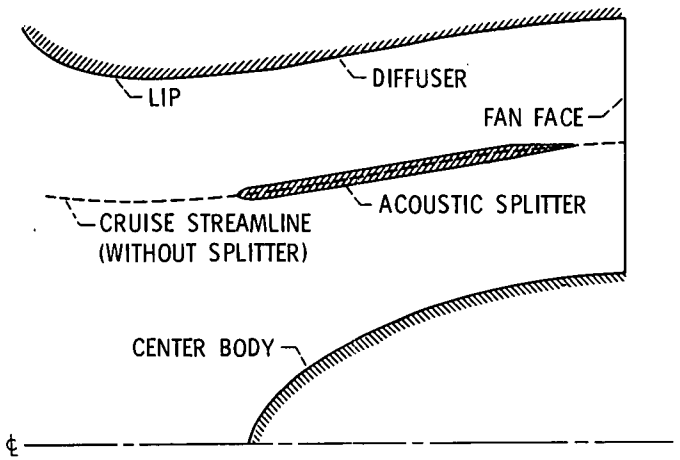

(a) INLET AND SPLITTER GEOMETRY.

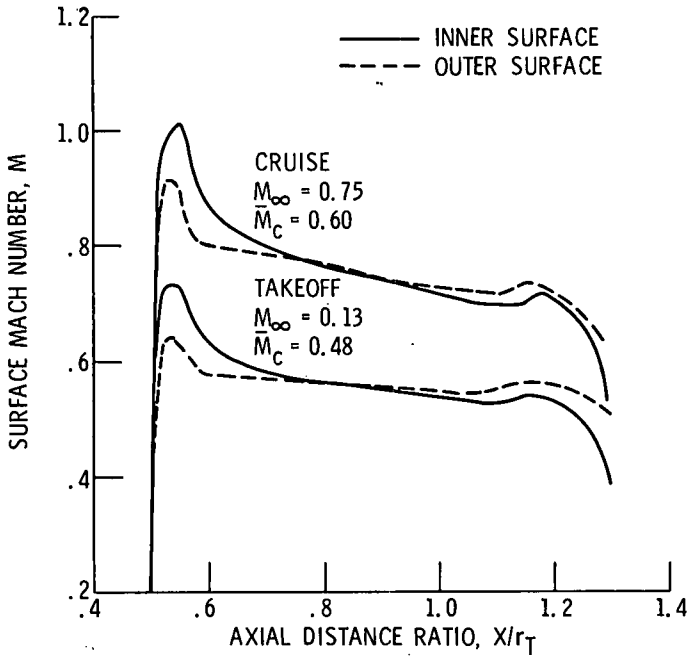

(b) MACH NUMBER DISTRIBUTIONS ON ACOUSTIC SPLITTER.

Figure 14. - Application of theory to acoustic splitter design.

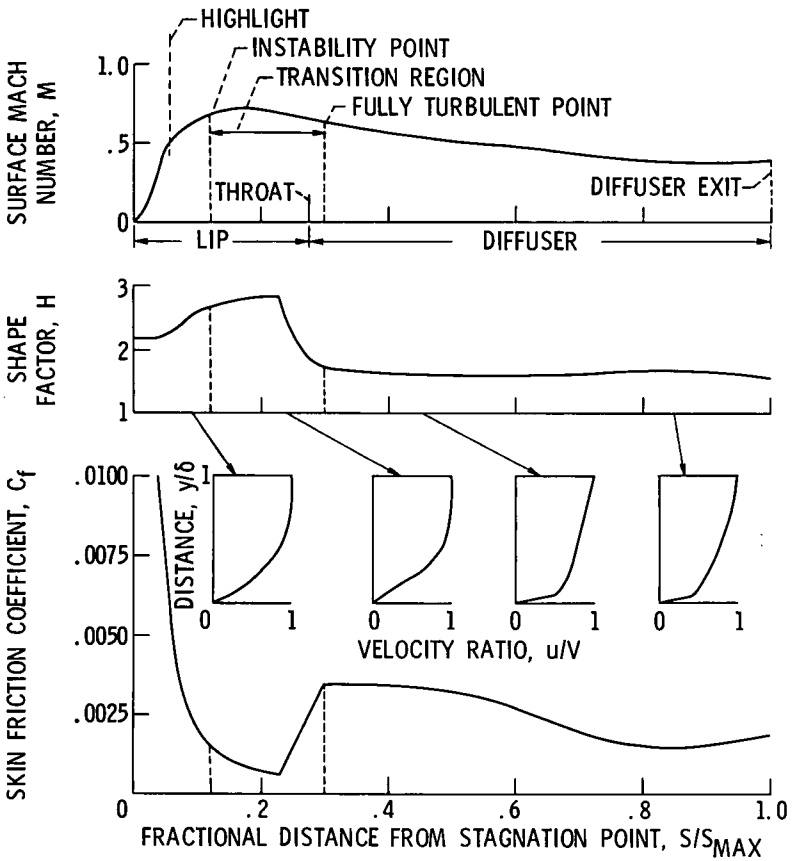

Figure 15. - Boundary layer characteristics on internal inlet surface for attached flow condition; free-stream velocity, V_∞, 45 m/sec; incidence angle, α, 0^0.

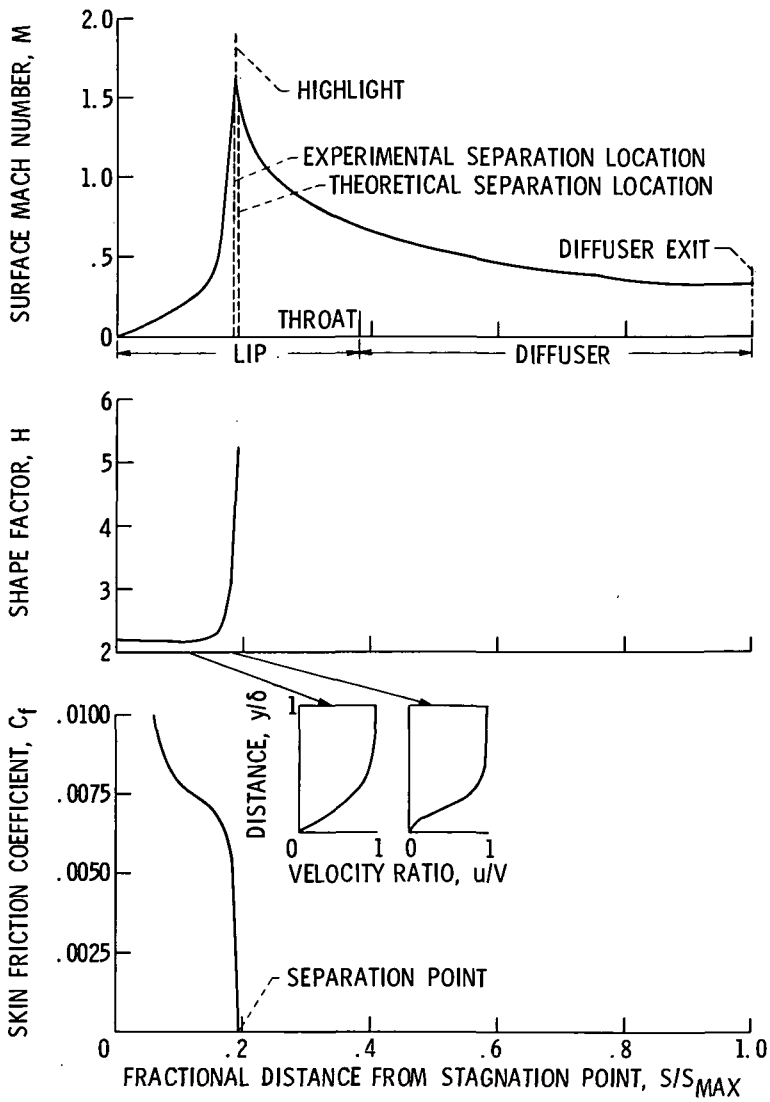

Figure 16. - Boundary layer characteristics on internal inlet surface for separated flow condition, free-stream velocity, V_∞, 45 m/sec; incidence angle, α, 50^0; windward side of inlet.